ELSEVIER

Journal of Molecular Structure (Theochem) 633 (2003) 123–136

THEO CHEM

www.elsevier.com/locate/theochem

Calculation of ring-current susceptibilities for potentially homoaromatic hydrocarbons

Jonas Jusélius, Michael Patzschke, Dage Sundholm*

Department of Chemistry, University of Helsinki, P.O. Box 55 (A.I. Virtasen Aukio 1), Helsinki FIN-00014, Finland

Received 30 September 2002; revised 29 November 2002; accepted 18 December 2002

Abstract

The degree of aromaticity of neutral and charged cyclic and potentially homoaromatic hydrocarbon species ($C_mH_{m+1}^q$, $m = 4–13$, $q = -1, 0, 1, 2$) with ($4n + 2$; $n = 0, 1, 2$) π electrons have been studied by calculating the magnetic shieldings in selected points. The ring-current susceptibility with respect to an external magnetic field has been estimated by employing the aromatic ring-current shielding (ARCS) method. The calculations show that the long-range magnetic shieldings provide information about the aromatic properties of the nonplanar molecules. The degree of aromaticity has also been estimated from nucleus-independent chemical shifts (NICS), bond-length alternations, and ^{1}H-NMR shieldings. The study indicates that $C_8H_9^{1+}$, $C_9H_{10}^{2+}$, $C_{10}H_{11}^{1-}$, and $C_{12}H_{13}^{1+}$ can be considered homoaromatic using the four criteria.
© 2003 Elsevier B.V. All rights reserved.

Keywords: Ab initio; Density functional theory; Aromaticity; Homoaromaticity; Ring current; Magnetic shielding

1. Introduction

Homoaromatic molecules are classified as compounds that show aromatic character even though the molecular conjugation is interrupted by single bonds [1–3]. The concept of homoaromaticity was introduced more than 40 years ago and it still awakens interest [3]. A family of potentially homoaromatic molecules can be derived from cyclic and conjugated ($4n + 2$) π-electron hydrocarbon species by inserting a CH_2 unit into the molecular ring. The best-known example of this kind of species is probably the homotropylium cation ($C_8H_9^{1+}$) which can be considered as a $C_7H_7^{1+}$ ion with an additional CH_2 unit. The homotropylium cation, also called homotropenylium, was isolated for the first time in 1962 [4]. The evidence for its aromaticity was based on measurements of the ^{1}H-NMR spectrum [4,5]; the NMR resonances of the *endo* and *exo* hydrogens at the C_8 carbon were found to be separated by 5.86 ppm. Since then, the homoaromaticity concept has been the subject for many computational studies [6–17]. Even though the degree of homoaromaticity is difficult to assess experimentally, there are many experimental studies of potentially homoaromatic molecules. See for example the review articles written by Childs [2] and Williams [3]. The homoaromaticity concept has also been much debated since it has proven to be even more

* Corresponding author. Tel.: +358-9-19150176; fax: +358-9-19140169.
E-mail address: sundholm@chem.helsinki.fi (D. Sundholm).

0166-1280/03/$ - see front matter © 2003 Elsevier B.V. All rights reserved.
doi:10.1016/S0166-1280(03)00267-7

difficult to find a unique criterion for homoaromaticity than for aromaticity [2,3,14,18].

The aim of this work is to estimate the degree of homoaromaticity of neutral and charged cyclic homoaromatic hydrocarbon species ($C_mH_{m+1}^q$, $m = 4–13$, $q = -1, 0, 1, 2$) with ($4n + 2$; $n = 0, 1, 2$) π electrons by calculating the magnetic shielding at selected points in the vicinity of the molecules. The magnetic shielding in these points can be divided into long-range and short-range contributions. The short-range contribution is due to the local motion of the electrons around the atoms and in the chemical bonds, whereas the long-range magnetic shielding is a result of induced ring currents in the delocalized π-electron system. For homoaromatic molecules a through space interaction between the C1 and C($n - 1$) carbons renders the ring current possible. The short-range contribution to the magnetic shielding vanishes with the electron density outside the molecule, whereas the magnetic shielding due to the ring current declines more slowly. This implies that the strength of the ring current, or more correctly the ring-current susceptibility, of aromatic molecules can be estimated by studying the long-range magnetic shielding as a function of the distance from the ring [19].

In the aromatic-ring-current-shielding (ARCS) method, the magnetic shielding in the selected points is obtained from quantum chemical calculations, whereas the electric current can be modeled by using classical electrodynamics [19]. The ARCS method has previously been employed for studies of induced ring currents in fused-ring molecules and for assessing the degree of aromaticity [19–24].

A popular approach for computational studies of molecular aromaticity is the nucleus-independent-chemical-shifts (NICS) method [25,26]. For comparison, we also use calculated NICS values, bond-length alternations, as well as ^{1}H-NMR and ^{13}C-NMR shieldings for assessing the aromaticity of the molecules studied. However, for studies of homoaromatic molecules, the NICS results are not always unambiguous since the choice of the position for the NICS point of ruffled molecules is somewhat arbitrary.

2. The ARCS method

An external magnetic field (B_{ext}) applied on a molecular species introduces movements of the electronic charges, i.e. it creates currents in the electron density. The currents are strong in those regions of space where the charge density is large; the currents are mainly localized at the nuclei. For cyclic conjugated molecules, the current can circulate around the whole molecular ring in the delocalized electron cloud [27–39]. Currents in turn induce magnetic fields (B_{ind}). The strong local currents at the nuclei are observed in NMR spectroscopy as chemical shifts, whereas due to the large loop radius, the current in the molecular ring (I_{ring}) creates long-range magnetic shieldings; the long-range shieldings are usually observed in ^{1}H-NMR spectra as small additional shifts in NMR resonances of the neighbor hydrogens. The strength of the induced magnetic field can be estimated from classical electrodynamics using Biot-Savart's law for an infinitely thin conductor wire [40]

$$d\mathbf{B} = \frac{\mu_0 I_{ring}}{4\pi} \frac{d\mathbf{l} \times \mathbf{r}}{r^3} \tag{1}$$

where μ_0 is the permeability of vacuum, $d\mathbf{l}$ is a small length element of the conductor, r is the distance from the wire, and $\mathbf{r}$ is the radial vector from $d\mathbf{l}$ to the probe. For an infinitely thin and circular wire, the expression for the induced magnetic field strength perpendicular to the current loop becomes

$$B(z)_{ind} = \frac{\mu_0 I_{ring}}{2} \frac{R^2}{(z^2 + R^2)^{3/2}} = -\sigma(z) B_{ext} \tag{2}$$

where R is the radius of the current loop, z is the perpendicular distance from the loop center, $\sigma(z)$ is the z-dependence of the isotropic magnetic shielding function, and B_{ext} is the applied magnetic field. Differentiation of Eq. (2) yields a relation between $\sigma(z)$ and the ring-current susceptibility with respect to the external magnetic field ($\partial I_{ring}/\partial B_{ext}$)

$$\sigma(z) = -\frac{\mu_0}{2} \frac{\partial I_{ring}}{\partial B_{ext}} \frac{R^2}{(z^2 + R^2)^{3/2}} \tag{3}$$

In the ARCS approach, the magnetic shieldings are calculated in discrete sample points along the z axis. The z axis is defined as the axis with the largest

moment of inertia. The current susceptibility and the current radius can be obtained by fitting the long-range part of the shielding function to Eq. (3). This can be done by adjusting the loop radius R until the angular coefficient in the logarithmic representation becomes 3/2. The current susceptibility can then be deduced from the intercept of the fitted line. In the ARCS fit, the estimated center of the current loop is chosen as the origin. For nonplanar molecules, the choice of origin is not quite unambiguous. However, the value of ring-current susceptibility has not proven to be very dependent on the precise location of the ARCS origin. The negative value of the magnetic shielding at the ARCS origin is the reported NICS value.

3. Computational methods

The molecular structures were optimized at the resolution-of-the-identity density-functional theory (RI-DFT) level [41] using the Becke-Perdew (BP) functional [42–44] as implemented in TURBOMOLE [45]. The magnetic shieldings have been calculated at the Hartree–Fock self-consistent-field (SCF) level [46,47]. To ensure origin-independence in the shielding calculations, gauge-including atomic orbitals have been employed [28,48–50]. In the structure optimization, the Karlsruhe split-valence basis sets (SV(P)) [51] augmented with polarization functions on C were used, whereas in the shielding calculations, the basis set was augmented with polarization functions on H (SVP). The ring-current susceptibilities and the radius of the current loop have been deduced from the long-range magnetic shieldings using the ARCS approach as described in Section 2.

The molecular structures optimized at the BP SV(P) level were checked by performing second-order Møller-Plesset (MP2) level calculations using split-valence (SVP) and triple-zeta (TZVP) [52] quality basis sets. In the MP2 optimizations, the resolution of the identity approach (RI-MP2) was employed [53–55]. The nuclear magnetic shieldings were also calculated at the MP2 level [47] using the SVP and TZVP basis sets.

4. Results

4.1. Molecular structures

The molecular structures were optimized as described in Section 3. The obtained stationary points were checked by calculating the vibrational frequencies. The molecular structures depicted in Figs. 1–11 are local minima since their vibrational frequencies are real. The large rings are flexible and for them we obtained more than one local minimum. For $C_{11}H_{12}$, the ruffled molecular structure shown in Fig. 8 is the energetically lowest one found. The severe ruffling of the molecular ring and the strong bond-length alternation indicate that it lacks molecular conjugation and homoaromaticity. $C_{12}H_{13}^{1+}$ was found to form chair and boat conformations. The chair conformation being lower in energy by 17 kJ mol^{-1}. For the small rings we obtained only one minimum corresponding to the boat conformation. An exception is C_7H_8 for which two isomers can be obtained [56,57]; a double ring structure with a three-member ring fused to an almost planar six-member ring (bicyclo[4.1.0]hepta-2,4-diene or norcaradiene) was found to lie higher in energy than the nonplanar structure (1,3,5-cycloheptatriene or tropilidene) shown in Fig. 4. For $C_{13}H_{14}^{2+}$, we found that the energetically lowest conformation consists of three fused rings (two five-member rings fused to a seven-member ring) with C_s symmetry. This structure is 91 kJ mol^{-1} lower in energy than a ruffled one-ring structure of C_1 symmetry. A ruffled one-ring structure of C_s symmetry lies energetically only 3.5 kJ mol^{-1} above the C_1 structure. Since the larger rings are flexible and can therefore easily form fused-ring structures and ruffled rings, it is not reasonable to extend the present study to larger species than $C_{13}H_{14}^{2+}$.

To check the basis-set and correlation effects on the molecular structures, we performed MP2 calculations on C_7H_8. As seen in Table 1, the obtained BP SV(P) structures are in fair agreement with those obtained at the MP2 level. There is no reason to expect any large basis-set and correlation contributions to the molecular structures of the other molecules, either. The Cartesian coordinates of the molecules can be downloaded from our world-wide-web (www) server [58].

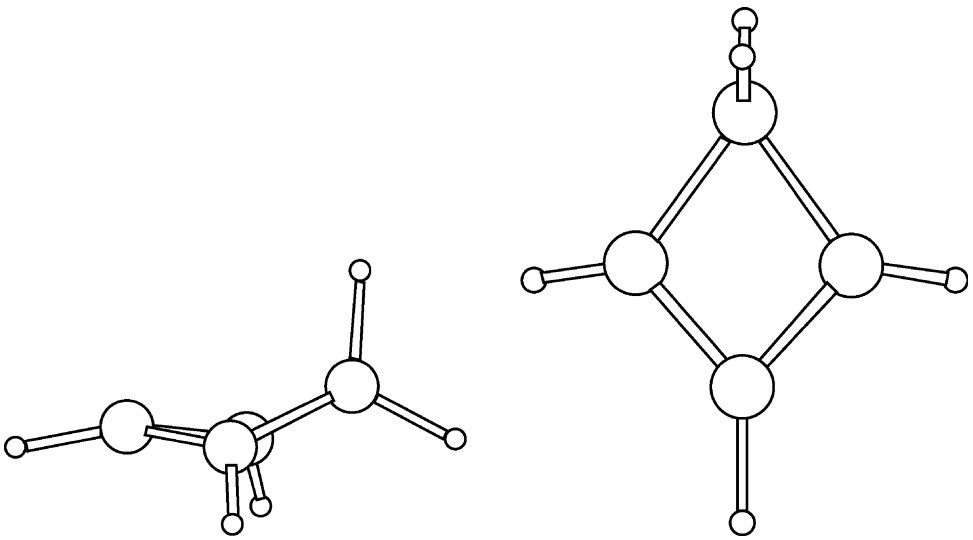

Fig. 1. The side and top view of the optimized molecular structure of $C_4H_5^{1+}$.

One measure of molecular aromaticity is the degree of bond-length alternation [59,60]. The C–C distances of the optimized structures are given in Table 2. The neutral C_7H_8 and $C_{11}H_{12}$ molecules have large bond length alternations of 7–9 pm, whereas for $C_8H_9^{1+}$, $C_9H_{10}^{2+}$, and $C_{12}H_{13}^{1+}$ the lengths of the C–C bonds are almost equal. For the molecules with small bond-length alternation the C1–C($n-1$) distance is about 200 pm. These observations indicate that $C_8H_9^{1+}$, $C_9H_{10}^{2+}$, and $C_{12}H_{13}^{1+}$ are homoaromatic, whereas the degree of homoaromaticity for the rest of the molecules must be estimated using other criteria.

4.2. Ring currents

The ring-current susceptibility (in nA T^{-1}) and the corresponding current radius (in pm) for the studied molecules are summarized in Table 3. NICS values as well as ARCS and NICS aromaticity indices are also

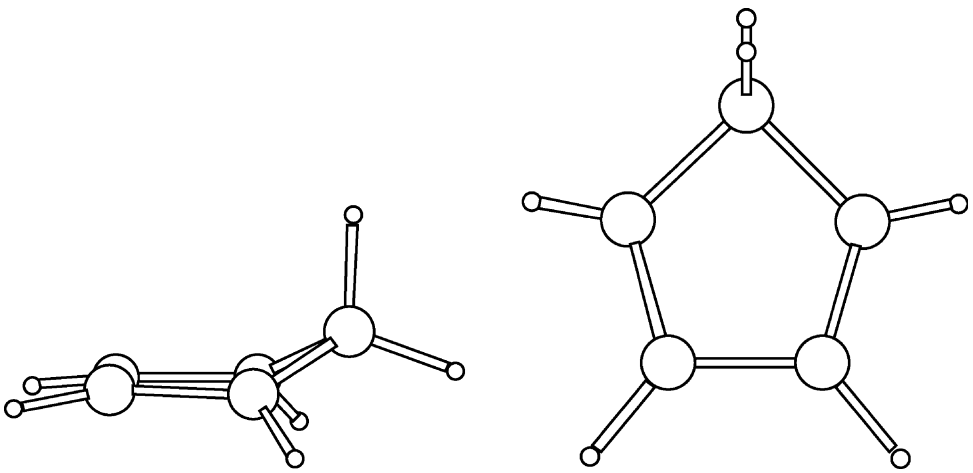

Fig. 2. The side and top view of the optimized molecular structure of $C_5H_6^{2+}$.

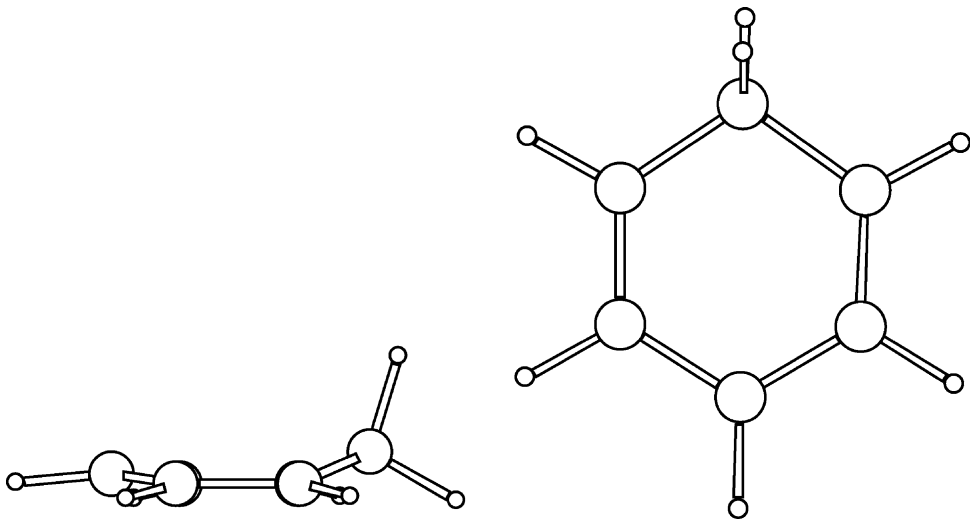

Fig. 3. The side and top view of the optimized molecular structure of $C_6H_7^{1-}$.

given. The ARCS aromaticity index is defined as the ring-current susceptibility relative to the benzene value calculated at the same level of theory. Analogously, the NICS aromaticity index is the NICS value relative to the corresponding NICS value for benzene. Note that the sign convention for NICS and ARCS values differ; negative NICS values [25] and positive ring-current susceptibilities indicate diatropic ring currents which often are used as a measure for the degree of aromaticity. Our experience is that a molecule with an ARCS index larger than 0.3 can be considered aromatic, whereas to determine the degree of aromaticity for a molecule with a small ARCS index, the long-range shielding function must be studied in more detail. The long-range magnetic shielding functions and the ARCS plots can be obtained from our www server [58].

The ARCS calculations show that $C_8H_9^{1+}$ and $C_9H_{10}^{2+}$ sustain ring currents that are almost twice the strength of the ring current for benzene. Judged from

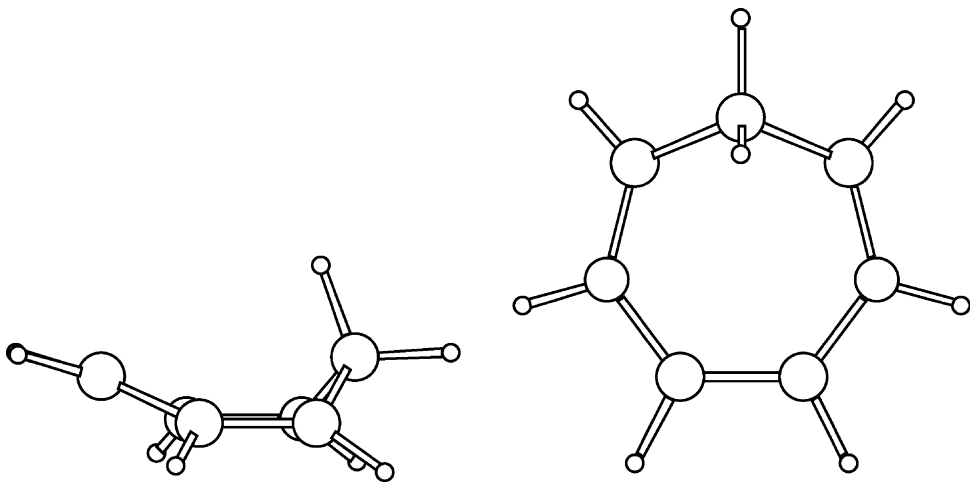

Fig. 4. The side and top view of the optimized molecular structure of C_7H_8.

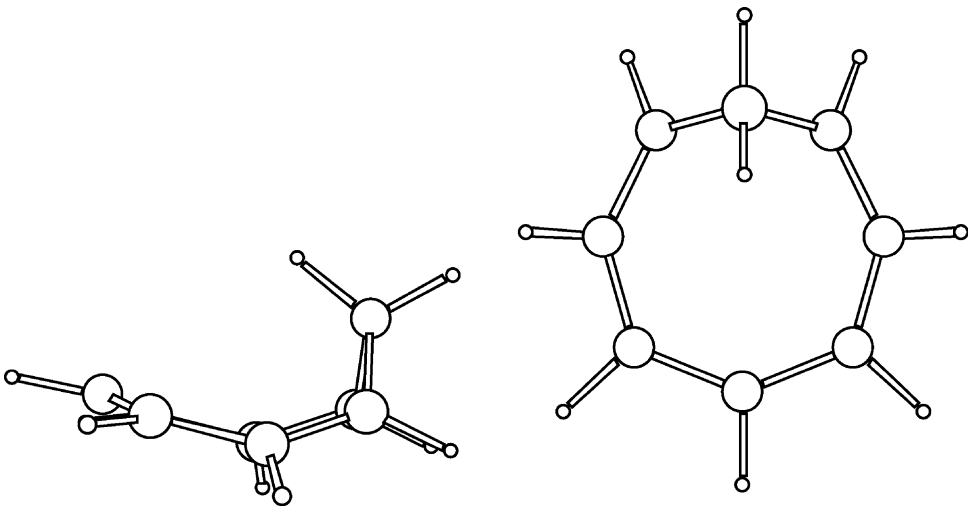

Fig. 5. The side and top view of the optimized molecular structure of $C_8H_9^{1+}$.

the ARCS index, other homoaromatic molecules are $C_{12}H_{13}^{1+}$, $C_5H_6^{2+}$, $C_{10}H_{11}^{1-}$, and $C_4H_5^{1+}$. The boat conformation of $C_{12}H_{13}^{1+}$ has a significantly larger current susceptibility than the chair conformation. The molecular rings of the $C_{13}H_{14}^{2+}$ of C_1 and C_s symmetry does not sustain any current, and for the $C_{13}H_{14}^{2+}$ conformation consisting of fused rings, the five-member ring sustains a weak ring current, whereas the seven-member ring is completely non-aromatic. The ARCS calculations show that $C_6H_7^{1-}$, $C_{11}H_{12}$, and $C_{13}H_{14}^{2+}$ are no candidates for homoaromatic molecules.

For the strongly homoaromatic molecules, the NICS values qualitatively show the same trends as obtained in the ARCS calculations. For the large rings, both the NICS and the ARCS calculations identify the same molecules as homoaromatic. However, the degree of aromaticity differs by about a factor of two. For C_7H_8, the NICS index of 0.49 is three times larger than the ARCS index. For $C_5H_6^{2+}$,

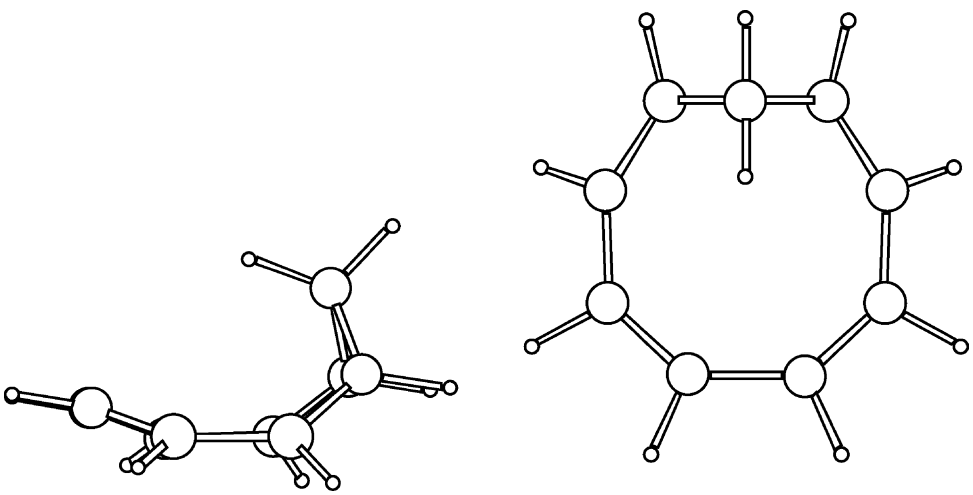

Fig. 6. The side and top view of the optimized molecular structure of $C_9H_{10}^{2+}$.

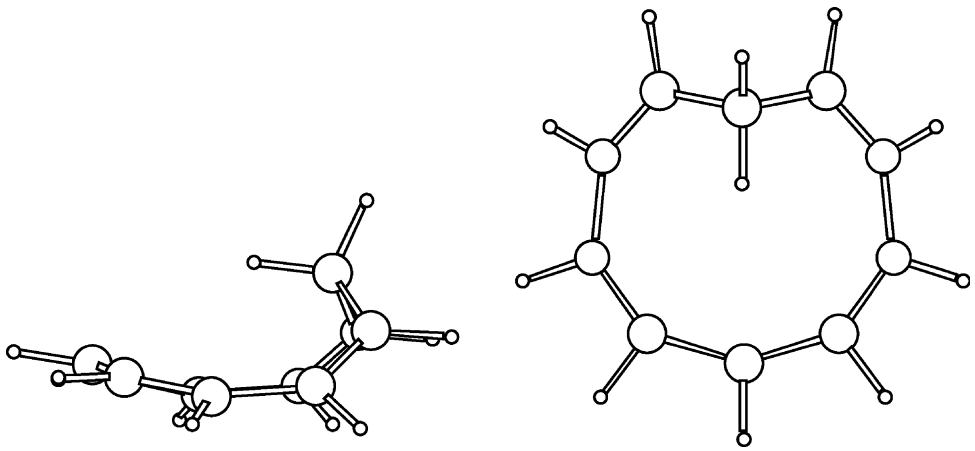

Fig. 7. The side and top view of the optimized molecular structure of $C_{10}H_{11}^{-}$.

the ARCS and NICS indices are of opposite sign. A close look at the ARCS function in Fig. 12 reveals that the magnetic shielding close to the ring center is paratropic indicating that it is an antiaromatic species, whereas the long-range shielding clearly shows that the ring sustains a diatropic current.

For the small molecules, the ring-current susceptibilities were calculated at the MP2 level. In general, the electron correlation effects did not alter the obtained results. However, for $C_4H_5^{1+}$, the ARCS index obtained at the MP2 level is almost a factor of four larger than at the SCF level.

The ARCS values given in Table 3 are obtained from the open side of the ring where the CH_2 group is not interfering. The long-range magnetic shielding function along the opposite direction of the z-axis is for many of the molecules severely perturbed by the presence of the *endo* hydrogen (Fig. 12).

4.3. Nuclear magnetic shieldings

The homoaromatic hydrocarbon species are non-planar with one of the CH_2 hydrogens pointing inwards (*endo*) and the *exo* hydrogen lies outside

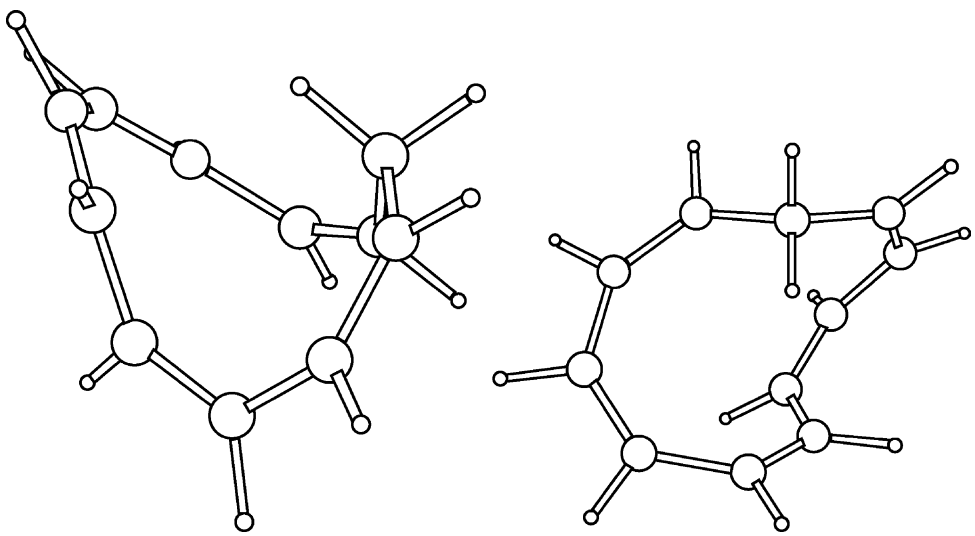

Fig. 8. The side and top view of the optimized molecular structure of $C_{11}H_{12}$.

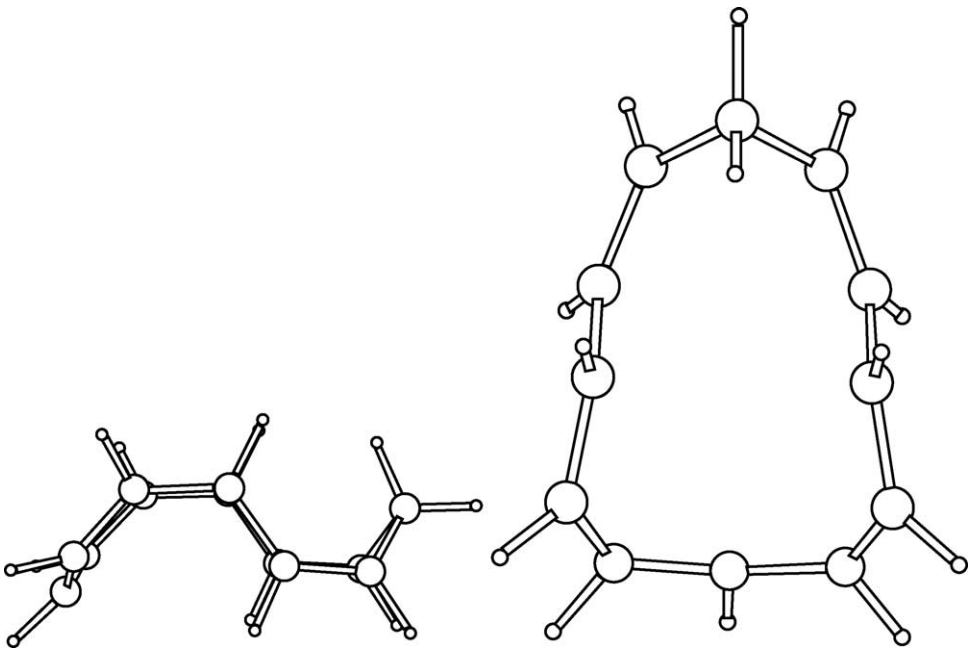

Fig. 9. The side and top view of the optimized molecular structure of $C_{12}H_{13}^{1+}$ (chair).

the current loop. In homoaromatic molecules, the ring current increases the ^{1}H-NMR shielding of the *endo* hydrogen and decreases the ^{1}H-NMR shielding of the *exo* hydrogen. The ^{1}H-NMR shieldings calculated at the SCF SVP level using the BP SV(P) molecular structure (SCF SVP/BP SV(P)) are given in Table 4. The small rings are stiff, thereby directing both the CH_2 hydrogens to the outside of the current loop. This can be observed in the *endo*–*exo* ^{1}H-NMR shielding difference. For the small molecules, the *endo*–*exo* shielding difference is negative. For the large molecules, sustaining a ring current, the shielding of

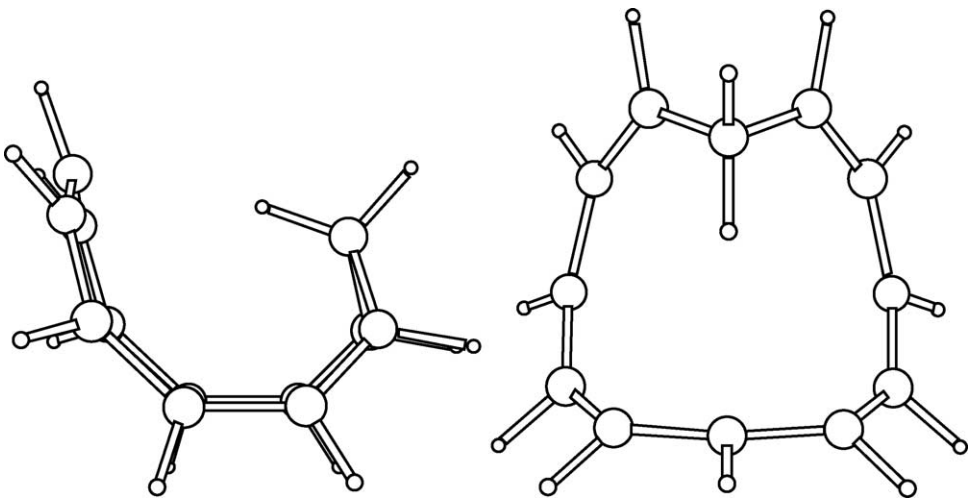

Fig. 10. The side and top view of the optimized molecular structure of $C_{12}H_{13}^{1+}$ (boat).

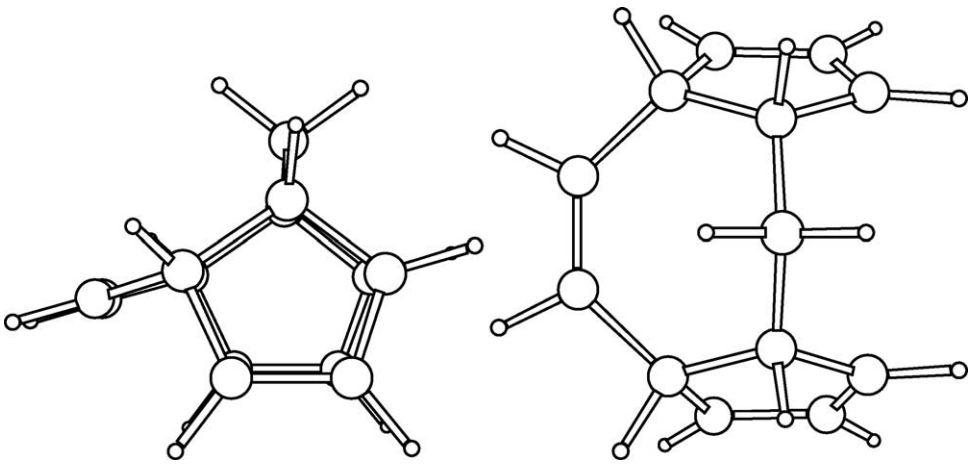

Fig. 11. The side and top view of the optimized molecular structure of $C_{13}H_{14}^{2+}$ with the lowest energy.

the *endo* hydrogen is larger than for the *exo* hydrogen. For $C_8H_9^{1+}$, the ^{1}H-NMR chemical shift between the *endo* and *exo* hydrogens is measured to be 5.86 ppm [2,3,5] as compared to the present value of 6.3 ppm obtained at the SCF SVP/BP SV(P) level. The ^{1}H-NMR resonance of the *exo* hydrogen measured on the isolated homotropylium salt occurs at $\delta = -0.73$ ppm relative to tetramethylsilan (TMS) [4], whereas semi-empirical calculations of the ^{1}H-NMR shieldings for a $C_8H_9^+$ molecule in gas phase [2] indicated that the *exo* hydrogen is shielded by $\delta = 1.5$ ppm relative to TMS. However, the present calculations show that for a single $C_8H_9^+$ molecule in gas phase, the ^{1}H-NMR resonance is deshielded by $\delta = 1.2$ ppm relative to TMS. Thus, the present value for the ^{1}H-NMR chemical shift of the *exo* hydrogen deviates by only 0.5 ppm from the experimental result. This tiny difference is likely due to vibrational, temperature, and solvent effects, which have not been considered in our calculations.

Table 1
A comparison of the C–C distances (in pm) for C_7H_8 calculated at the BP and MP2 levels using different basis sets

Method	Basis set	C1–C7	C1–C2	C2–C3	C3–C4	C1–C6
BP	SV(P)	151.1	136.7	144.7	138.2	243.0
BP	SVP	151.0	136.6	144.7	138.2	242.9
BP	TZVP	150.7	135.8	144.2	137.3	242.1
MP2	SVP	149.9	136.3	144.2	137.7	239.2
MP2	TZVP	149.7	135.5	143.7	137.0	238.4

As seen in Table 4, the ^{1}H-NMR chemical shifts of the hydrogens attached to the unsaturated carbons are not a very accurate indicator for homoaromaticity. However, for $C_8H_9^{1+}$ and $C_9H_{10}^{2+}$ with large ring radii and strong ring currents, these hydrogens are more shielded than one in general observes for nonaromatic conjugated molecules.

The calculations of the ^{13}C-NMR shieldings show that, for the homoaromatic molecules sustaining a strong ring current, the chemical shifts of the unsaturated carbons are almost equal (see also Ref. [3]). For the apparently nonaromatic molecules, the ^{13}C-NMR shieldings alternate. However, as seen in Table 5, there are many exceptions; the ^{13}C-NMR chemical shifts are not an accurate measure of the degree of homoaromaticity.

In Tables 6 and 7, the ^{1}H-NMR and ^{13}C-NMR chemical shifts (in ppm) relative to TMS are given and compared to available experimental results. The magnetic shieldings have been calculated at the SCF TZVP/BP SV(P) and MP2 TZVP/BP SV(P) levels. To render comparisons with measured NMR spectra possible, the ^{1}H-NMR and ^{13}C-NMR shieldings for TMS were calculated at the same levels of theory. At the SCF TZVP/BP SV(P) level, we obtained for TMS ^{1}H-NMR and ^{13}C-NMR shieldings of 31.5 and

Table 2
The C–C distances (in pm) for the studied $C_mH_{m+1}^q$ hydrocarbon species calculated at the BP SV(P) level

Molecule	Cn–C1	C1–C2	C2–C3	C3–C4	C4–C5	C5–C6	C6–C7	C1–C(n − 1)
$C_4H_5^{1+}$	151	140						176
$C_5H_6^{2+}$	150	145	140					215
$C_6H_7^{1-}$	152	139	143					248
C_7H_8	151	137	145	138				243
$C_8H_9^{1+}$	149	140	141	141				203
$C_9H_{10}^{2+}$	150	141	141	142	142			196
$C_{10}H_{11}^{1-}$	150	138	143	141	143			233
$C_{11}H_{12}$ [a]	151	137	146	138	145			256
$C_{12}H_{13}^{1+}$ [b]	150	140	141	141	141	143		198
$C_{12}H_{13}^{1+}$ [c]	150	141	141	141	141	141		192
$C_{13}H_{14}^{2+}$	155	149	140	140	149	153	135	266

The carbon atoms are numbered starting from the first unsaturated carbon (C1) and ending at the saturated carbon (Cn).
[a] The obtained structure does not belong to the C_s point group. The corresponding bond distances for the second half of the ring are 152, 136, 146, 137, and 145 pm, respectively.
[b] The chair conformation (see Fig. 9).
[c] The boat conformation (see Fig. 10).

196.8 ppm, respectively, and at the MP2 TZVP/BP SV(P) level, they are 31.3 and 194.4 ppm, respectively.

The ^{1}H-NMR and ^{13}C-NMR chemical shifts calculated at the MP2 TZVP/BP SV(P) level are in rather close agreement with measured ones. For the hydrogens, the calculated and measured chemical shifts agree within 0.5 ppm, whereas the ^{13}C-NMR chemical shifts differ only a few ppm from the experimental results. The largest discrepancies were

Table 3
The geometrical ring radius (in pm), the effective current radius (in pm), the induced ring-current susceptibility (in nA T^{-1}), the NICS value (in ppm) calculated at the center of mass, and the ARCS and NICS aromaticity indices relative to benzene

Molecule	R(geom.)[a]	R(current)	$\partial I_{ring}/\partial B$	NICS	ARCS index	NICS index
$C_4H_5^{1+}$ SCF	88	121	3.6	−18.6	0.45	1.74
$C_4H_5^{1+}$ MP2		57	13.7	−17.8	1.54	2.00
$C_5H_6^{2+}$ SCF	113	138	4.3	+1.4	0.53	−0.13
$C_5H_6^{2+}$ MP2, b		108	6.2	+1.1	0.70	−0.12
C_7H_8 SCF	153	217	1.2	−5.2	0.15	0.49
C_7H_8 MP2		225	1.4	−5.4	0.16	0.61
$C_8H_9^{1+}$ SCF	164	100	14.7	−13.4	1.84	1.25
$C_9H_{10}^{2+}$ SCF	184	110	14.9	−11.3	1.86	1.06
$C_{10}H_{11}^{1-}$ SCF	218	208	3.8	−9.0	0.47	0.84
$C_{12}H_{13}^{1+}$ SCF, c	175	209	3.8	−19.1	0.48	1.79
$C_{12}H_{13}^{1+}$ SCF, d	193	174	10.0	−12.8	1.25	1.20
$C_{13}H_{14}^{2+}$ SCF, e	120	166	2.5	−2.2	0.28	0.21

The ARCS value for benzene calculated at the same level is 8.0 ppm. [d]The NICS value for benzene calculated at the same level is −10.7 ppm.
[a] The geometrical radius is estimated from the C–C distance across the ring.
[b] The corresponding ARCS and NICS values for benzene are 8.9 and −8.9 ppm, respectively.
[c] The chair conformation (see Fig. 9).
[d] The boat conformation (see Fig. 10).
[e] The five-member ring (see Fig. 11).

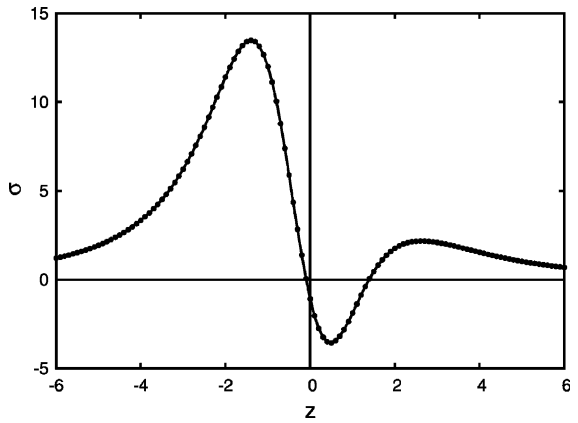

Fig. 12. The magnetic shielding function (in ppm) along the z-axis for $C_5H_6^{2+}$.

obtained for $C_6H_7^-$. For anions, the solvent and counter-ion effects on magnetic shieldings can be substantial. Large deviations from measured ^{13}C-NMR shifts were also obtained for the C1 atoms, probably due to the omitted vibrational contributions.

4.4. Neutral homoaromatic molecules

The existence of neutral homoaromatic molecules has been a much debated subject [3,18,61–63]. Cycloheptatriene (C_7H_8), which would be the homoaromatic analog of benzene, is one of the candidates for neutral homoaromatic molecules. The optimized molecular structure has a large alternation of the C–C bonds. The aromaticity index obtained from ARCS calculations indicates that the degree of aromaticity is about one-sixth of the benzene value. The chemical shift difference between the ^{1}H-NMR signals of the *exo* and *endo* hydrogens calculated at different levels of theory are given in Table 8. The chemical shift difference of 1.38 ppm obtained at the SCF SVP/BP SV(P) level is in perfect agreement with the experimental result [64,65], whereas calculations at the more accurate levels of theory yield *endo*–*exo* shifts of about 2 ppm; the main reason for the discrepancy is likely the vibrational corrections.

The long-range magnetic shielding function indicates that C_7H_8 is a weakly homoaromatic molecule. Herges and Geuenich [63] reported explicit calculations of the ring current for C_7H_8. In the plot of the anisotropy of the current-induced density (ACID), the through space interaction between C1 and C6 carbons is indeed seen. Thus, in an external magnetic field a weak ring current is induced into the molecular ring, but the calculations show that the ring current is not very strong.

Table 4
The ^{1}H-NMR magnetic shieldings (in ppm) calculated at the SCF SVP/BP SV(P) level

Molecule	Hn(*endo*)	Hn(*exo*)	H1	H2	H3	H4	H5	H6
$C_4H_5^{1+}$	26.6	27.7	23.9	21.5				
$C_5H_6^{2+}$	24.7	25.2	19.0	20.6				
$C_5H_6^{2+}$ MP2	24.1	25.2	19.1	20.6				
$C_6H_7^{1-}$	28.0	28.8	29.5	26.3	29.6			
C_7H_8	30.3	29.0	26.4	25.5	25.0			
$C_8H_9^{1+}$	32.9	26.6	25.2	23.4	22.7	23.1		
$C_9H_{10}^{2+}$	32.7	25.2	23.3	21.7	21.3	21.4		
$C_{10}H_{11}^{1-}$	33.9	31.1	26.8	26.5	27.6	25.4	27.6	
$C_{11}H_{12}$	29.1	29.5	26.4	26.3	26.0	25.8	25.5	
$C_{11}H_{12}$ [a]			26.5	25.6	25.5	26.2	25.7	
$C_{12}H_{13}^{1+}$ [b]	34.1	30.7	24.1	24.3	24.8	23.7	23.5	24.2
$C_{12}H_{13}^{1+}$ [c]	31.2	27.5	26.2	27.3	27.3	24.1	23.8	23.8
$C_{13}H_{14}^{2+}$ [d]	28.4	28.2	27.9	20.9	23.5	20.8	27.3	25.2

[a] The shieldings for the corresponding hydrogens of the second half of the molecule with a nearly C_s symmetry.
[b] The chair conformation (see Fig. 9).
[c] The boat conformation (see Fig. 10).
[d] The fused-ring structure (see Fig. 11).

Table 5
The ^{13}C-NMR magnetic shieldings (in ppm) calculated at the SCF SVP/BP SV(P) level

Molecule	C1	C2	C3	C4	C5	C6	Cn
$C_4H_5^{1+}$	60	7					153
$C_5H_6^{2+}$	−73	8					137
$C_5H_6^{2+}$ MP2	−69	1					117
$C_6H_7^{1-}$	124	54	135				165
C_7H_8	76	70	62				173
$C_8H_9^{1+}$	73	48	44	52			164
$C_9H_{10}^{2+}$	36	17	32	29			152
$C_{10}H_{11}^{1-}$	98	76	108	62	111		175
$C_{11}H_{12}$	56	70	63	69	65		170
$C_{11}H_{12}$ [a]	68	65	65	54	57		
$C_{12}H_{13}^{1+}$ [b]	97	49	40	43	62	33	171
$C_{12}H_{13}^{1+}$ [c]	85	53	51	65	63	49	173
$C_{13}H_{14}^{2+}$ [d]	148	−49	57	−52	146	70	173

[a] The shieldings for the corresponding hydrogens of the second half of the molecule with a nearly C_s symmetry.
[b] The chair conformation (see Fig. 9).
[c] The boat conformation (see Fig. 10).
[d] The fused-ring structure (see Fig. 11).

The NICS calculation yields an aromaticity index of 0.49 suggesting that C_7H_8 is a rather homoaromatic molecule. This value can be compared to the ARCS aromaticity index of only 0.15.

Table 6
The ^{1}H-NMR chemical shifts (in ppm) relative to tetramethylesilane (TMS) calculated at the SCF TZVP/BP SV(P) and MP2 TZVP/BP SV(P) levels as compared to experimental data

Molecule	Method	Hn(*endo*)	Hn(*exo*)	H1	H2	H3	H4
$C_4H_5^{1+}$	SCF	4.96	3.90	7.71	10.04		
	MP2	4.91	3.87	7.47	9.43		
	Exp.[a,b]	4.53	4.53	7.95	9.72		
$C_6H_7^{1-}$	SCF	4.61	3.97	2.78	5.57	2.17	
	MP2	5.37	4.79	2.92	5.00	2.49	
	Exp.[a,c]	3.4	3.4	3.3	5.9	3.7	
C_7H_8	SCF	1.24	2.64	5.35	6.23	6.72	
	MP2	1.14	2.93	4.94	6.24	6.60	
	Exp.[d]	1.31	2.69	5.27	6.09	6.50	
$C_8H_9^{1+}$	SCF	−1.24	4.97	6.48	8.31	8.97	8.53
	MP2	−1.20	5.23	6.02	8.53	8.57	8.52
	Exp.[e]	−0.73	5.13	6.48	8.39	8.57	8.27

[a] The *endo* and *exo* shifts are thermally averaged.
[b] See Ref. [66] and references therein.
[c] See Ref. [67].
[d] See Ref. [64].
[e] See Ref. [5].

Table 7
The ^{13}C-NMR chemical shifts (in ppm) relative to tetramethylesilane (TMS) calculated at the SCF TZVP/BP SV(P) and MP2 TZVP/BP SV(P) levels as compared to experimental data

Molecule	Method	C1	C2	C3	C4	Cn
$C_4H_5^{1+}$	SCF	141.9	197.0			47.8
	MP2	131.1	188.8			55.3
	Exp.[a]	133.5	187.6			54.0
$C_6H_7^{1-}$	SCF	81.4	149.9	60.2		34.5
	MP2	78.3	129.0	67.9		41.6
	Exp.[b]	75.8	131.8	78.0		30.0
C_7H_8	SCF	126.9	133.5	140.6		25.6
	MP2	112.9	127.4	131.3		31.3
	Exp.[c]	120.4	126.8	131.0		28.1
$C_8H_9^{1+}$	SCF	129.1	155.8	159.0	151.0	34.7
	MP2	114.2	156.3	142.9	148.4	41.6
	Exp.[d]	121.6	153.1	144.6	144.1	43.1

[a] See Ref. [66]. Paquette [68] reported chemical shifts of 130 and 188 ppm for C1 and C2, respectively.
[b] See Ref. [67].
[c] See Ref. [69].
[d] See Ref. [70]. The ^{13}C chemical shifts were measured relative to CS_2; its chemical shift relative to TMS is 193.1 ppm [71].

5. Summary

The magnetic shieldings have been calculated for a family of potentially homoaromatic hydrocarbon species ($C_mH_{m+1}^q$, $m = 4$–13, $q = -1$, 0, 1, 2). The obtained shieldings have been used for assessing the degree of aromaticity for the molecules studied. The degrees of aromaticity have been estimated by performing ARCS and NICS calculations as well as calculations of ^{1}H-NMR shieldings. Bond-length alternation has also been used as one measure for

Table 8
The *endo*–*exo* chemical shift difference (in ppm) for C_7H_8 calculated at different levels of theory as compared to experiment

Structure	Shielding	H7(*endo*)–H7(*exo*)
BP SV(P)	SCF SVP	1.38
MP2 SVP	SCF SVP	1.67
MP2 SVP	MP2 SVP	2.05
MP2 TZVP	SCF TZVP	1.65
MP2 TZVP	MP2 TZVP	2.09
Experiment[a]	Experiment	1.38

[a] Refs. [64,65].

Table 9
The relative degree of aromaticity obtained at the SCF level using the different criteria

Rank	Bond alternation[a]	ARCS index	NICS index	^{1}H-NMR[b]
1	$C_{12}H_{13}^{1+c}$	$C_9H_{10}^{2+}$	$C_{12}H_{13}^{1+d}$	$C_9H_{10}^{2+}$
1		$C_8H_9^{1+}$		$C_8H_9^{1+}$
2	$C_8H_9^{1+}$		$C_4H_5^{1+}$	
3	$C_9H_{10}^{2+}$	$C_{12}H_{13}^{1+c}$	$C_8H_9^{1+}$	$C_{12}H_{13}^{1+c}$
4	$C_{12}H_{13}^{1+d}$	$C_{12}H_{13}^{1+d}$	$C_{12}H_{13}^{1+c}$	$C_{12}H_{13}^{1+d}$
5		$C_5H_6^{2+}$	$C_9H_{10}^{2+}$	$C_{10}H_{11}^{1-}$
6		$C_{10}H_{11}^{1-}$	$C_{10}H_{11}^{1-}$	C_7H_8
7		$C_4H_5^{1+}$	C_7H_8	

[a] Smallest bond-length alternation.
[b] Largest *endo–exo* shift.
[c] The boat conformation (see Fig. 10).
[d] The chair conformation (see Fig. 9).

aromaticity. The relative degrees of aromaticity obtained in this study are summarized in Table 9. The calculations show that 3–6 of the studied molecules can be considered homoaromatic depending on the criteria used. The most homoaromatic ones are $C_8H_9^{1+}$ and $C_9H_{10}^{2+}$, which seem to have about the same degree of aromaticity. $C_{12}H_{13}^{1+}$ can also be considered homoaromatic using the four criteria. No other molecules are ranked as homoaromatic species by all these criteria. The ARCS index indicates that $C_4H_5^{1+}$ and $C_5H_6^{2+}$ sustain diatropic currents, whereas NICS calculations suggest that C_7H_8 belongs to the class of homoaromatic molecules. The difference in the ^{1}H-NMR shieldings for the *endo* and *exo* hydrogens and the shape of the long-range shielding function indicate that C_7H_8 is weakly homoaromatic. The large *endo–exo* shifts of 6.3, 7.5, 2.8, and 2.9 ppm show that at least $C_8H_9^{1+}$ and $C_9H_{10}^{2+}$, $C_{10}H_{11}^{1-}$, and $C_{12}H_{13}^{1+}$ can be considered homoaromatic. Interestingly, a C1–C($n-1$) distance of about 200 pm seems to be a good indication of homoaromaticity.

The comparison of the degrees of aromaticity given in Table 9 shows that the ARCS method and the ^{1}H-NMR shieldings find the same molecules to be the most aromatic. The bond-alternation criterion yields the same ranking but in a slightly different order, whereas the NICS approach apparently has some difficulties in assessing the degree of homoaromaticity. For slightly homoaromatic molecules or for homoaromatic molecules with a small ring size, the ARCS method is the method of choice.

Acknowledgements

The generous supports by The Academy of Finland and the University of Helsinki's Research Funds are acknowledged. We acknowledge the support from the European research training network on 'Molecular Properties and Molecular Materials' (MOLPROP), contract No. HPRN-2000-00013. We also thank Prof. R. Ahlrichs for a copy of TURBOMOLE.

References

[1] S. Winstein, J. Am. Chem. Soc. 81 (1959) 6524.
[2] R.F. Childs, Acc. Chem. Res. 17 (1984) 347.
[3] R.V. Williams, Chem. Rev. 101 (2001) 1185.
[4] J.L. von Rosenberg Jr., J.E. Mahler, R. Petit, J. Am. Chem. Soc. 84 (1962) 2842.
[5] P. Warner, D.L. Harris, C.H. Bradley, S. Winstein, Tetrahedron Lett. 11 (1970) 4013.
[6] W.L. Jorgensen, J. Am. Chem. Soc. 98 (1976) 6784.
[7] E. Kaufmann, H. Mayr, J. Chandrasekhar, P. von Ragué Schleyer, J. Am. Chem. Soc. 103 (1981) 1375.
[8] J.B. Grutzner, W.L. Jorgensen, J. Am. Chem. Soc. 103 (1981) 1372.
[9] R.C. Haddon, J. Am. Chem. Soc. 110 (1988) 1108.
[10] P. Svensson, F. Reichel, P. Ahlberg, D. Cremer, J. Chem. Soc. Perkin Trans. 2 (1991) 1463.
[11] D. Cremer, F. Reichel, E. Kraka, J. Am. Chem. Soc. 113 (1991) 9459.
[12] R. Willershausen, C. Kybart, N. Stamatis, W. Massa, M. Bühl, P. von Ragué Schleyer, A. Berndt, Angew. Chem. Int. Ed. Engl. 31 (1992) 1238.
[13] D. Cremer, P. Svensson, E. Kraka, Z. Konkoli, P. Ahlberg, J. Am. Chem. Soc. 115 (1993) 7457.
[14] H. Jiao, N.J.R. van Eikema Hommes, P. von Ragué Schleyer, A. de Meijere, J. Org. Chem. 61 (1996) 2826.
[15] R. Nishinaga, Y. Izukawa, K. Komatsu, J. Phys. Org. Chem. 11 (1998) 475.
[16] C. Lepetit, C. Godard, R. Chauvin, New J. Chem. 25 (2001) 572.
[17] D. Scheschkewitz, M. Hofmann, A. Ghaffari, P. Amseis, C. Präsang, W. Mesbah, G. Geiseler, W. Massa, A. Berndt, J. Organometallic Chem. 646 (2002) 262.
[18] K.N. Houk, R. Wells Gandour, R.W. Strozier, N.G. Rondan, L.A. Paquette, J. Am. Chem. Soc. 101 (1979) 6797.
[19] J. Jusélius, D. Sundholm, Phys. Chem. Chem. Phys. 1 (1999) 3429.
[20] J. Jusélius, D. Sundholm, Phys. Chem. Chem. Phys. 2 (2000) 2145.

[21] J. Jusélius, D. Sundholm, J. Org. Chem. 65 (2000) 5233.
[22] J. Jusélius, D. Sundholm, Phys. Chem. Chem. Phys. 3 (2001) 2433.
[23] J. Jusélius, M. Straka, D. Sundholm, J. Phys. Chem. A 105 (2001) 9939.
[24] R.J.F. Berger, M.A. Schmidt, J. Jusélius, D. Sundholm, P. Sirsch, H. Schmidbaur, Z. Naturforsch. b 56 (2001) 979.
[25] P. von Ragué Schleyer, C. Maerker, A. Dransfeld, H. Jiao, N.J.R. van Eikema Hommes, J. Am. Chem. Soc. 118 (1996) 6317.
[26] G. Subramanian, P. von Ragué Schleyer, H. Jiao, Angew. Chem. Int. Ed. Engl. 35 (1996) 2638.
[27] L. Pauling, J. Chem. Phys. 4 (1936) 637.
[28] F. London, J. Phys. Radium 8 (1937) 397.
[29] J.A. Pople, J. Chem. Phys. 24 (1956) 1111.
[30] J.A. Pople, Mol. Phys. 1 (1958) 175.
[31] R. McWeeny, Mol. Phys. 1 (1958) 311.
[32] J.A. Elvidge, L.M. Jackman, J. Chem. Soc. (1961) 859.
[33] R.J. Abraham, R.C. Sheppard, W.A. Thomas, S. Turner, Chem. Comm. (1965) 43.
[34] W. Kutzelnigg, C. van Wüllen, U. Fleischer, R. Franke, T.V. Mourik, Nuclear Magnetic Shieldings and Molecular Structure, in: J.A. Tossell (Ed.), Kluwer Academic Publishers, Drodrecht, 1993, pp. 141–161.
[35] V.I. Minkin, M.N. Glukhovtsev, B.Y. Simkin, Aromaticity and Antiaromaticity—Electronic and Structural Aspects, Wiley, New York, 1994.
[36] U. Fleischer, W. Kutzelnigg, P. Lazzeretti, V. Mühlenkamp, J. Am. Chem. Soc. 116 (1994) 5298.
[37] M. Bilde, A. Hansen, Mol. Phys. 92 (1997) 237.
[38] I. Morao, F.P. Cossío, J. Org. Chem. 64 (1999) 1868.
[39] P. Lazzeretti, Prog. Nucl. Magn. Res. Spectr. 36 (2000) 1.
[40] G. Arfken, Mathematical Methods for Physicists, Academic Press, Orlando, 1985.
[41] K. Eichkorn, O. Treutler, H. Öhm, M. Häser, R. Ahlrichs, Chem. Phys. Lett. 240 (1995) 283.
[42] S.H. Vosko, L. Wilk, M. Nusair, Can. J. Phys. 58 (1980) 1200.
[43] J.P. Perdew, Phys. Rev. B 33 (1986) 8822.
[44] A.D. Becke, Phys. Rev. A 38 (1988) 3098.
[45] R. Ahlrichs, M. Bär, M. Häser, H. Horn, C. Kölmel, Chem. Phys. Lett. 162 (1989) 165.
[46] M. Häser, R. Ahlrichs, H.P. Baron, P. Weis, H. Horn, Theoret. Chim. Acta 83 (1992) 551.
[47] M. Kollwitz, M. Häser, J. Gauss, J. Chem. Phys. 108 (1998) 8295.
[48] H. Hameka, Mol. Phys. 1 (1958) 203.
[49] R. Ditchfield, Mol. Phys. 27 (1974) 789.
[50] K. Wolinski, J.F. Hinton, P. Pulay, J. Am. Chem. Soc. 112 (1990) 8251.
[51] A. Schäfer, H. Horn, R. Ahlrichs, J. Chem. Phys. 97 (1992) 2571.
[52] A. Schäfer, C. Huber, R. Ahlrichs, J. Chem. Phys. 100 (1994) 5829.
[53] D. Feller, E.D. Glendening, D.E. Woon, M.W. Feyereisen, J. Chem. Phys. 103 (1995) 3526.
[54] M.W. Feyereisen, D. Feller, D.A. Dixon, J. Phys. Chem. 100 (1996) 2993.
[55] F. Weigend, M. Häser, Theoret. Chem. Acc. 97 (1997) 331.
[56] J.M. Schulman, R.L. Disch, M.L. Sabio, J. Am. Chem. Soc. 106 (1984) 7696.
[57] F. Liebman, A. Skancke, Mol. Phys. 91 (1997) 471.
[58] http://www.chem.helsinki.fi/ ~ sundholm/qc/homoaromatic
[59] A. Julg, P. François, Theoret. Chim. Acta 8 (1967) 249.
[60] K. Jug, A. Köster, J. Phys. Org. Chem. 4 (1991) 163.
[61] R.V. Williams, H.A. Kurtz, J. Org. Chem. 53 (1988) 3626.
[62] W.H. Donovan, W.E. White, J. Org. Chem. 61 (1996) 969.
[63] R. Herges, D. Geuenich, J. Phys. Chem. A 105 (2001) 3214.
[64] H. Günther, NMR Spectroscopy, Wiley, New York, 1980.
[65] M. Schindler, W. Kutzelnigg, J. Am. Chem. Soc. 105 (1983) 1360.
[66] G.A. Olah, J.S. Staral, R.J. Spear, G. Liang, J. Am. Chem. Soc. 97 (1975) 5489.
[67] G.A. Olah, G. Asensio, H. Mayr, P. von Ragué Schleyer, J. Am. Chem. Soc. 100 (1978) 4347.
[68] L.A. Paquette, Angew. Chem. Int. Ed. Engl. 90 (1978) 114.
[69] H. Günther, NMR Spectroscopy, Wiley, New York, 1995.
[70] L.A. Paquette, M.J. Broadhurst, P. Warner, G.A. Olah, G. Liang, J. Am. Chem. Soc. 95 (1973) 3386.
[71] W. Gombler, Z. Naturforsch. 36B (1981) 1561.